Fire Safety Journal 161 (2026) 104664

Contents lists available at ScienceDirect

Fire Safety Journal

journal homepage: www.elsevier.com/locate/firesaf

A CFD fire simulation model for external living walls

Fuchen Jia, Zhaozhi Wang, Edwin R. Galea *, John Ewer

Centre for Safety, Resilience and Protective Security, University of Greenwich, 30 Park Row, Greenwich, London, UK

ARTICLE INFO

Keywords:
Living wall
Green wall
CFD
Modelling
SBI fire test
BS8414 fire test
Large scale fire test

ABSTRACT

A CFD fire model for Living Walls (LW) is presented in this paper. The combustion of the LW support structure (plastic material) is modelled as an external cladding system within SMARTFIRE. The plants and growing medium of the LW system are represented as two groups of combustible porous materials, which consist of solid particles. The combined model provides a unique capability to simulate fires in external LW systems and is validated using data from a variety of LW fire experiments. The model produced good agreement for the measured HRR in an SBI fire test; comparable burning states and temperature profiles of two large-scale tests; and similar time to fail for a LW structure, without plants or growth media, in a BS 8414 test. It is found that although the simulated HRRs from the burning plants are sensitive to the moisture content, the plant mass, the surface area to volume ratio etc., the total HRR of the investigated LW system is dominated by the burning of the plastic structure. It is suggested that the fire risk posed by the investigated LW system is at least as high as that for a Grenfell type cladding system.

Nomenclature

t	Time (s)
Cp_s	Specific heat of solid plant or growing medium particles (J/kgK)
HRR	Heat release rate (kW)
LW	Living wall
Q_{conv}	Gas/particle convective heat transfer (W)
Q_{rad}	Gas/particle radiative heat transfer (W)
Q_s	Energy absorbed and released in the solid phase including moisture evaporation, pyrolysis and char oxidation (J)
$Y_{s,C}$	Mass fraction of char of solid particles
$Y_{s,H2o}$	Moisture content of solid particles
$Y_{s,W}$	Mass fraction of dry wood of solid particles
SA/V	Surface area to volume ratio of solid particles (1/m)
T_g	Temperature of the gas mixture (K)
T_s	Temperature of solid particles (K)
α_s	Volume fraction of solid plant or growing medium particles
ρ_s	Density of solid plant or growing medium particles (kg/m^3)
σ_s	Surface area/volume (SA/V) ratio of solid particles
$\vartheta_{ash}, \vartheta_C, \vartheta_S$	Mass fraction of ash, char and soot
$\dot{\omega}_{s,C}$	Char formation rate (kg/s)
$\dot{\omega}_{s,H2o}$	Moisture evaporation rate (kg/s)
$\dot{\omega}_{s,W}$	Vegetation pyrolysis rate (kg/s)

1. Introduction

Living walls (LWs), also known as green walls, are vertical, vegetated structures consisting of modular panels or geotextile mats, which are fixed to external building facades or internal walls. There are many environmental, aesthetic and psychological drivers for LWs such as, bringing biodiversity to our urban environments, lessening the urban heat island effect, cleaning the air, dampening noise and providing a biophilic backdrop - which people require for health and wellbeing [1]. However, these compelling benefits cannot override the fundamental need to ensure that building fire safety is not compromised or reduced as a priority by the desire to reap the environmental benefits of LWs. As reviewed by Kotzen et al. [2] while there have been only a few reported LW fires, the fire safety risk posed by LWs is of concern, particularly due to the lack of appropriate fire test methods to assess the risk posed by a LW system. Currently, the SBI test (EN 13823) [3] is widely used to quantify the fire performance of LW systems by the LW industry. This subjects specimens to a 30 kW fire [3]. The BS 8414 fire test is magnitudes larger, subjecting specimens to a 3000 kW fire [4]. Although the BS 8414 fire test is recommended to assess external cladding wall systems, including LWs in the UK [5], it has not been used to assess LW systems, or at least there are no publicly available reports describing such applications. However, a LW structure BS 8414 test, which

This article is part of a special issue entitled: FISJ_IAFSS 2026 published in Fire Safety Journal.

* Corresponding author.
E-mail address: E.R.Galea@gre.ac.uk (E.R. Galea).

https://doi.org/10.1016/j.firesaf.2026.104664
Received 20 September 2025; Received in revised form 1 February 2026; Accepted 20 February 2026
Available online 21 February 2026

excluded plants and growing medium, has been conducted by the Fire Protection Association (FPA) [6]. The test shows that the LW structure fails the BS 8414 test in 130 s.

Assessments of the fire risk of LWs using CFD fire simulation are scarce in the literature. Dahanayake et al. [7] simulated fire development in a LW located in an underground corridor. In this study the LW is modelled as a common burnable wall with the ignition and spread of fire represented using heat release rates per unit area for three plant species, which are obtained from cone calorimeter tests. By treating a plant leaf as a single particle, Karunaratne et al. [8] explored the impact of moisture content and fuel packing ratio of vegetation on fire spread on vertical greenery systems using the pyrolysis model in FDS developed for vegetation. The model was based on the vegetation thermal degradation model and the Lagrangian particle model. In this model, the solid-phase thermal degradation process uses three reactions: the endothermic moisture evaporation, endothermic pyrolysis of dry vegetation and exothermic char oxidation. In the study by Karunaratne et al., a hypothetical building LW is considered which excludes the support structure for the LW. Using the same model, Karunaratne et al. also investigated experimentally and numerically the fire hazard associated with vertical greenery systems involving woodwool [9]. Unfortunately, the CFD simulations by Karunaratne et al., only consider the burning of plants, excluding the burning of plastic modules commonly found in LW systems; the module support systems; irrigation system; and physical structure of LW systems.

In this paper, a LW fire model is presented that utilises the SMARTFIRE CFD fire simulation environment. The model integrates a cladding fire model [10] and a shrub fuel bed model to simulate LW fires. The model is described in Section 2. A series of comprehensive validations of the integrated model are presented in Section 3 for the burning rate of a LW system, Section 4 for the impact of the moisture content in large-scale fires and Section 5 for the BS 8414 LW structure fire. The fire risk posed by a LW system is discussed in Section 6 by comparing its simulated performance in a BS8414 test with the that for an ACM (with PE core) cladding system. The limitations of the model are also discussed in this section. Finally, conclusions are presented in Section 7.

2. The model

A research version of SMARTFIRE V5.1 software [11] is the basis of the LW fire model. The CFD engine in SMARTFIRE has many physics features that are required for fire field modelling, that have been described previously many times in the literature [12–17], so their description is not repeated here. These sub-models include k-ε turbulence model; flame spread model; gaseous combustion model (eddy dissipation combustion model) [18]; smoke model, toxicity model, etc. It is specially noted that the radiative transfer equation is solved using the discrete ordinates method with 48 rays.

The CFD fire model for a LW system presented in this paper consists of two main components, the representation of the combustion of the LW support structure (plastic materials) and the representation of the combustion of the plants and growth medium. The combustion of the LW support system makes use of the previously developed cladding wall fire model [10]. In the cladding fire model, all combustible surfaces are assigned a face patch type which identifies them as a burnable material. Each face patch is labelled with a unique patch number which defines their location and material properties. At the end of each time step, conditions at a cell face of a potentially burnable face patch are assessed to determine if ignition conditions are reached. The ignition of the material is solely determined by the surface ignition temperature while other criteria such as critical heat flux and exposure duration being excluded. While this is a simplification, it has been shown to produce good results in previous studies [19]. Furthermore, the use of critical heat-flux and a required delay time to ignition cannot be employed in the current study for the investigated PP material as the heat-flux related cone calorimeter data [20] is unavailable. Once a cell face is ignited, it starts to release a certain amount of fuel according to the time dependent burning rate (kg/m^{2}s) or HRR for this material, for which data has been collected from small-scale tests. Once the solid material of the panel at a specific face cell is burnt off, a burn-through of the panel at the location occurs, which is modelled by the removal of this solid face cell. The burnt off solid face cells further affect the integrity of the cavity in the LW system.

The plants and growing medium of the LW system are represented as two groups of porous materials, which consist of solid particles. The solid particles are characterised by a set of physical properties including density, ratio of surface area to volume (SA/V), and moisture content. The variables $Y_{s,W}$, $Y_{s,H2o}$ and $Y_{s,C}$ denote the mass fraction of dry wood, moisture content, and char of solid particles respectively. The mass, species and energy conservation for the solid phase can be written as Equations (1)–(5) [21,22].

$$\frac{d(\alpha_s\rho_s Y_{s,H2o})}{dt} = -\dot{\omega}_{s,H2o} \tag{1}$$

$$\frac{d(\alpha_s\rho_s Y_{s,W})}{dt} = -\dot{\omega}_{s,W} \tag{2}$$

$$\frac{d(\alpha_s\rho_s Y_{s,C})}{dt} = (\vartheta_C - \vartheta_S)\dot{\omega}_{s,W} - \left(\frac{\vartheta_{ash}}{\vartheta_C} + 1\right)\dot{\omega}_{s,C} \tag{3}$$

$$\frac{d(\alpha_s)}{dt} = -\frac{1}{\rho_s}\dot{\omega}_{s,C} \tag{4}$$

$$\alpha_s\rho_s Cp_s\frac{dT_s}{dt} = Q_{conv} + Q_{rad} + Q_s \tag{5}$$

where α_s, ρ_s and Cp_s are volume fraction, density and specific heat of solid phase of the plant; $\dot{\omega}_{s,H2o}$ is moisture evaporation rate; $\dot{\omega}_{s,W}$ is vegetation pyrolysis rate; $\dot{\omega}_{s,C}$ is char formation rate. Q_{conv} is the convective heat transfer between gas and solid phases given by Equation (6),

$$Q_{conv} = h_{conv}\alpha_s\sigma_s(T_g - T_s) \tag{6}$$

where σ_s is surface to volume ratio of vegetation. Q_{rad} is radiative heat transfer given by Equation (7),

$$Q_{rad} = \frac{\alpha_s\sigma_s}{4}\left(Q_{ir} - 4\sigma T_s{}^4\right) \tag{7}$$

where Q_{ir} is the total irradiance. Q_s is the energy absorbed and released in the solid phase including moisture evaporation, pyrolysis and char oxidation. It is noted that char oxidation is not implemented in this study due to the lack of data.

The pyrolysis rate, $\dot{\omega}_{s,W}$, is the fuel release rate for the gas phase. Besides this gaseous fuel generated from the plants and growing medium, the wood crib fire source, and the burnable LW support also contribute gaseous fuels by pyrolysis in fires. In the gaseous combustion model, the molecular structure of wood ($C_1H_{1.7}O_{0.83}$) is used for all the combustible plants, growing medium and wood crib. For the combustion of LW structure, the molecular structure of $(C_3H_6)n$ is used in this study as the main LW structure material is polypropylene.

3. Simulation of one SBI test – validation I

In this section, the LW fire model is validated using data from one SBI test. The validation in this section focusses on the capability of the model to predict the HRR resulting from the burning of a LW. The model parameters used in the simulations described in this section and the simulations described in subsequent sections are summarised in Table 1 for the plants and growing medium and Table 2 for plastic materials for modules and the irrigation system. The surface area volume ratio (SA/V)

Table 1
Input model parameters for plants and growing medium.

Parameters	Unit	Value	
		Plant	Growing medium
SA/V	1/m	3000	60
Moisture content	%	284 [20]	100
Packing ratio	dimensionless	0.027	0.85
Heat of combustion	MJ/kg	13.18 [20]	12.27 [20]
Fuel region thickness	m	0.1	0.1
Density (dry)	Kg/m^3	480	880
Specific heat of plants	J/kgK	1110 [24]	1110
Pyrolysis heat for plants and growing medium	J/kg	418000 [22]	418000
Ignition temperature	K	400 [22]	400
Char fraction		0.2 [25]	0.1

Table 2
Input model parameters for module plastics.

Material	Density (kg/m^3)	Conductivity (W/mK)	Specific heat (J/kgK)	Ignition temperature (^{O}C)
PP	938 [26]	0.21 [26]	1930 [26]	210 [27]
PVC	1380 [28]	0.16 (0.13-0.19) [28]	1440 (1290-1590) [28]	415 [27]
Membrane (PVC)	1380	0.16	1440	257 [29]

for leaves is typically 4000/m [22]. However, considering the high moisture content of the LW, a value of 3000/m is applied in the simulations presented here. The dry plant mass of approximately 0.05 kg per module and density of 480 kg/m^3 are derived from the experimental data by Newcomer [23]. With an assumed plant region thickness of 0.1 m, a packing ratio of 0.027 is estimated. Most of the material properties for the specific plants (see Table 1) and the LW support structure (see Table 2) investigated in this study are unknown and so representative values are derived from the literature. Given the uncertainty in model parameters, a series of sensitivity studies are conducted as part of this study. This includes a sensitivity analysis related to plant model parameters moisture content, plant mass per module and SA/V. Furthermore, as the HRR from the LW support structure is demonstrated to dominate the total HRR for the system, a further sensitivity analysis is also conducted related to the material properties of the support system (PP) i.e., density, specific heat, conductivity and surface ignition temperature.

The HRRs (Fig. 1) from cone calorimeter experiments for PP, PVC and membrane are from the work Bielawski et al. [20], Hischler [30] and Blomqvist et al. [31].

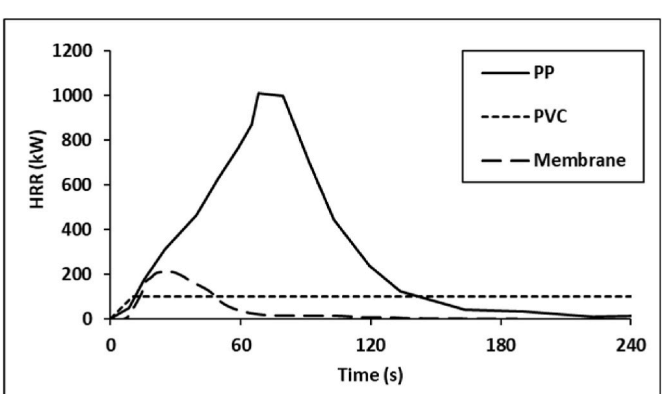

Fig. 1. HRR of PP, PVC and waterproof membrane.

3.1. The SBI test and simulation scenarios

The SBI LW experiment was conducted by Bielawskiet al. [20]. The LW module has dimensions of 0.5 × 0.25 × 0.1 m^3 and is made of fire retarded polypropylene (PP). The module pots are filled with substrate and vegetation are planted in them. Fig. 2 shows the LW system in the test, the CFD setup of the LW structure, i.e. the plastic modules, and the finished LW system including the growing medium and plants. According to the SBI protocol, the width of the shorter and longer wing of the wall was 0.5 m and 1.0 m respectively and the wall height is 1. 5 m. For safety reasons, the height of the specimen in the experiment was set to 1.0 m i.e., two modules high (see Fig. 2). There is a 0.05 m gap between the back of the LW module and the structural wall. The modelled plants extend 0.1 m from the outer face of the LW module.

A total of five scenarios are simulated.

- **Scenario S1**: the simulation of the SBI test [20] with model parameters in Table 1 and Table 2.
- **Scenario S2**: as S1, with an increase of the dry plant mass from 0.05 to 0.06 kg/module.
- **Scenario S3**: as S1, with a decrease of plant moisture content from 284% to 200%.
- **Scenario S4**: as S1, with a decrease of SA/V from 3000/m to 2400/m.
- **Scenario S5**: as S1, with density of 900 kg/m^3 (decrease of 3%), conductivity of 0.17 W/mK (decrease of 19%) and specific heat of 1900 J/kgK (decrease of 11%) for PP.
- **Scenario S6**: as S1, with an increase of PP ignition temperature from 210 ^{O}C to 305 ^{O}C.

The CFD simulations of the SBI test were performed using a computational mesh consisting of 277,760 (56 × 80 × 62) cells. A non-uniform mesh is utilised, with a cell size of 0.01 m within the plant region, 0.03 m just outside the plant region and 0.05 m at locations far away from the LW system. To support this mesh selection, a mesh sensitivity study was performed involving a mesh budget of 828,240 (87 × 112 × 85) computational cells. As seen in Fig. 3, the coarse mesh and the fine mesh produce almost identical overall heat release rate (HRR) for the LW system and quite close HRR curves for the plants. Using a computer with a 4.0 GHz ten-core processor and 128 GB of memory, it took approximately 37 h and 104 h to simulate an SBI scenario using the coarse and fine mesh budgets respectively. Considering six SBI simulation scenarios are explored in this study, the coarse mesh is adopted in all the simulations.

3.2. Burning rate of the SBI test

The measured and the predicted HRRs of the SBI LW fire are compared in Fig. 4. As seen in Fig. 4(a), after ignition started (at 300 s), the measured HRR quickly increases to a peak value of 244.2 kW at 485 s. The simulation successfully reproduces the measured trends up to 600 s, with the peak HRR under predicted by 29.8 kW or 12%. While the peak HRR of the SBI LW fire is as high as 244.2 kW, the predicted HRR from the burning of plants has a maximum of 12.9 kW (Fig. 4(b)), just 5.3% of the whole system. While the HRR of the investigated LW system is dominated by the LW structure, not the plants and the growing medium, the fire risk posed by plants in the LW should not be ignored. The plants could be considered as a wick, which can spread flame to other parts of the wall that may be vulnerable e.g., open windows or vents.

3.3. Sensitivity analysis

As seen in Fig. 4, the burning rate of the plants is sensitive to the model parameters used to represent the plants. With a decrease in the moisture content from 284% to 200% (Scenario S3), the LW fire develops just a few seconds sooner and the peak predicted burning rate of

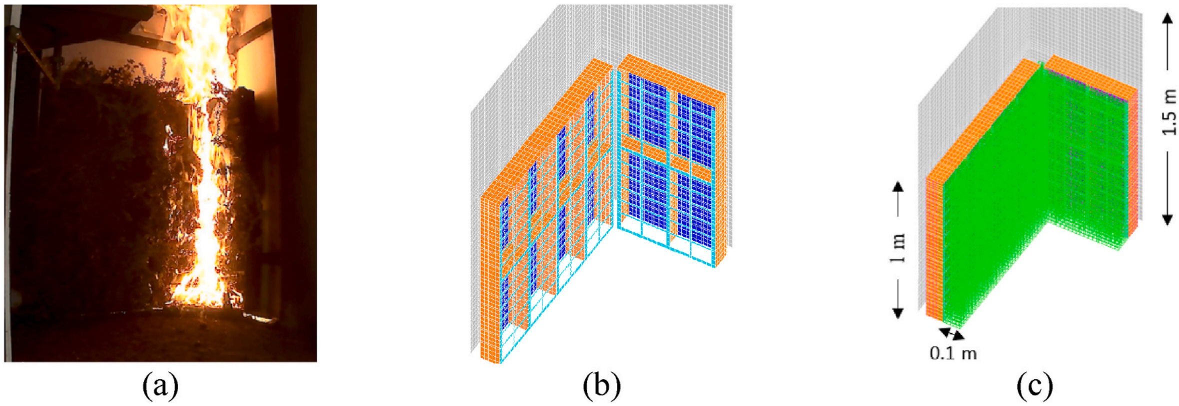

Fig. 2. (a) SBI LW fire experiment [20] and CFD setup of the (b) LW module structure and (c) final LW system.

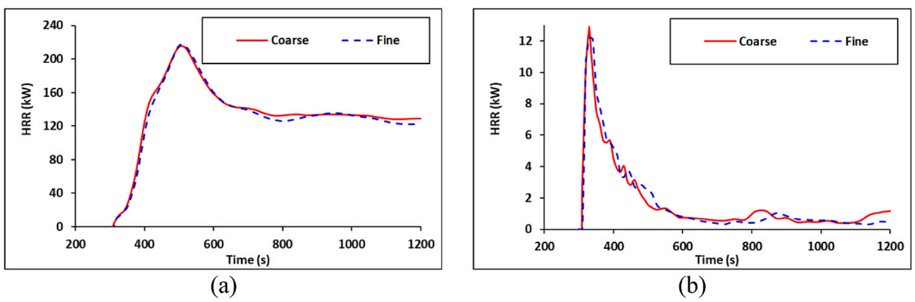

Fig. 3. Simulated HRRs of (a) the LW system and (b) the plants in the SBI test, with the coarse mesh and fine mesh.

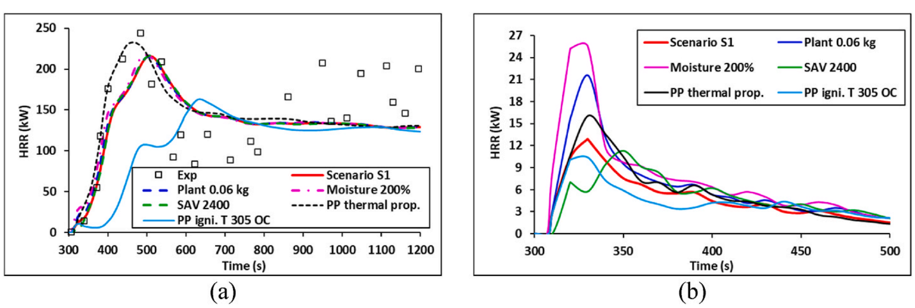

Fig. 4. Measured and predicted burning rates of (a) the LW system and (b) the plants and medium of SBI test in various simulation scenarios.

the plants increases from 12.9 kW to 25.5 kW or 98% (Fig. 4(b)). With an increase in the dry plant mass from 0.05 kg per module to 0.06 kg per module (Scenario S2), the peak HRR increases from 12.9 kW to 21.6 kW or 67%. A decrease of the SA/V ratio from 3000/m to 2400/m (Scenario S4) results in a clear delay in the ignition of the plants and the predicted peak burning rate decreases from 12.9 kW to 10.5 kW or 9%. While the burning rate of the plants is sensitive to the related model parameters (Fig. 4 (b)), their impact on the overall predicted HRRs of the LW system is minor (Fig. 4(a)). This supports the suggestion that the main fire risk of the investigated LW product is dominated by the plastic structure, not the plants.

It is noted that some commercial PP materials have a slightly lower density and specific heat to that assumed in Scenarios S1 to S4. In Scenario S5, the density of the PP is decreased from 938 kg/m^3 to 900 kg/m^3 or 4%, the specific heat is decreased from 1900 J/kgK to 1700 J/kgK or 11%, and the conductivity is decreased from 0.21 W/mK to 0.17 W/mK or 19%. The resulting predicted HRRs over the first 600 s are in good agreement with the measured data (Fig. 4(a)), with a peak HRR of 232.7 kW, compared with the experimental value of 244.2 kW and base case (Scenario S1) of 215.8 kW. The surface ignition temperature of 210 ^{O}C for PP utilised in Scenarios S1 to S5 is derived from a calculation based on cone calorimeter data [27], where the measured surface ignition temperatures vary between 250 ^{O}C and 360 ^{O}C. A simulation using a surface ignition temperature midway between the range of measured temperatures i.e., 305 ^{O}C (Scenario S6) delays the fire spread over the LW system and produces a peak HRR of 162.5 kW, which under-predicts the measured data by 81.7 kW or 33%. However, after 600 s, the different surface ignition temperatures produce similar HRRs.

4. Simulations of large-scale fire tests – validation II

In this section, the LW fire model is further validated with data from two large fire tests. This validation focuses on the model capability to predict the fire characteristics impacted by plant moisture content.

4.1. Large-scale LW fire tests and simulations

The two large LW fire tests with wet and dry plants are conducted by Bielawskiet al. [20]. The LW in the large tests are 2.5 m high and 1.75 m wide, including 35 LW modules. The fire source was wood cribs consisting of eight layers stacked alternately with a total weight of approximately 20 kg. The wooden elements with two types of geometry, measuring 0.6 m × 0.04 m × 0.04 m and 0.3 m × 0.04 m × 0.04 m. The average HRR of the burning crib was estimated to be 249.4 kW. The moisture content of the wet plants is 284% (see Table 1), while for the dry plants, it is 9%. Four thermocouples at 1.5 m and 2.25 m high and 0.125 m from the symmetry line of the test wall were used to measure the temperatures within the plants. The precise location of the thermocouples from the surface of the LW module is not known, but the thermocouples are thought to be obscured by the plants. Within the model, the thermocouples are located in the middle of the plant region i.e., 0.05 m from the module surface. Due to the symmetry of the computational domain, only half of the geometry is considered in the simulations. Fig. 5 shows the model setup of the left half geometry. The plant model parameters are the same as those specified in the Scenario S1 simulation in Section 3 for the wet LW system.

For the dry LW, the change of moisture content from 284% (for wet LW) to 9% suggests that the plant volume is reduced to approximately one quarter of its original volume. It is also assumed that while the reduction of moisture content reduces the volume of plants, the impact on the surface area is negligible – at least for leaves. Therefore, the SA/V ratio is increased from 3000/m to 12000/m, which is quite close to the SA/V for grasses (i.e. 12240/m) [32]. The HRR for the wood crib fire increases quadratically to 249.4 kW in 360 s and then remains at this average value in the simulations. For these large-scale tests, a similar mesh density is used for the LW system as in the SBI fire simulations but with relatively large cells at remote locations from the LW. A mesh budget of 257,756 (37 × 133 × 56) computational cells is used to represent half of the geometry (exploiting symmetry in the physical fire test). A fire test duration of 1200 s is simulated.

4.2. Simulation results

It is not surprising that the fire spreads faster on the dry LW compared to the wet LW. As seen in Fig. 6(a), at 445 s for the wet LW, the fire is localised in the area above the wood crib. At a similar time (450 s), the fire has spread laterally to the middle point between the crib and the edge of the dry LW. In Fig. 6, the red dots represent the burning locations of the PP LW modules. The yellow contours represent the iso-surface of combustion intensity (0.4 MW/m^3) contributed from the burning of plants. Generally, the model produces an identifiably wider burning area in the dry LW than that in the wet LW. From the predicted HRRs in Fig. 7, the time to ignition of the plants in the dry LW is 160 s, some 100 s sooner than that for the wet plants. In addition, the peak HRR for the dry LW is 778.3 kW, some 11% higher than that for the wet LW and a second HRR peak value of 465.7 kW is also observed.

The measured [34] and predicted temperatures for the two tests are compared in Fig. 8. In the wet LW test, the measured temperatures at a height of 1.5 m gradually increased to a peak of 476.6 ^{O}C at 845 s. The predicted peak temperature is 731.8 ^{O}C, some 54% higher than the measured peak. It is noted that the predicted temperatures around the wet plants are very sensitive to location. The predicted temperatures at the same height as the thermocouples but at a distance not obscured by the plants (located 0.05 m from the plant surface) are similar to the measured data.

The difference between measured and predicted temperature could be due to the change in the physical structure of the plant bed due to deformation of the wet plants prior to burning, which changes the apparent thickness of the plant bed. This deformation behaviour, which is relevant for wet plants, but not dry plants, is not currently represented within the model. The predicted temperatures for the dry LW follow the measured trends reasonably well, with the peak predicted temperature at a height of 2.25 m being 760.5 ^{O}C, under predicting the measured value by 125.4 ^{O}C or 14.2%.

These results support the recommendation in Kotzen al [2]. that fire testing of a LW system should reflect the minimum acceptable state of the plants and growth medium (including moisture levels). In this way test results identify the expected performance of the maximum degraded LW system which is still considered acceptable.

5. Simulations of BS 8414 LW structure fire test – validation III

In this section, the capability of the LW fire model to simulate a LW structure fire is validated. The data is derived from a BS8414 test conducted by the Fire Protection Association (FPA) [6] of a LW structure without plants or growing medium. This scenario may represent the installation phase of the LW, and potentially at other times during the life of a LW installation where the plants and growing media are being

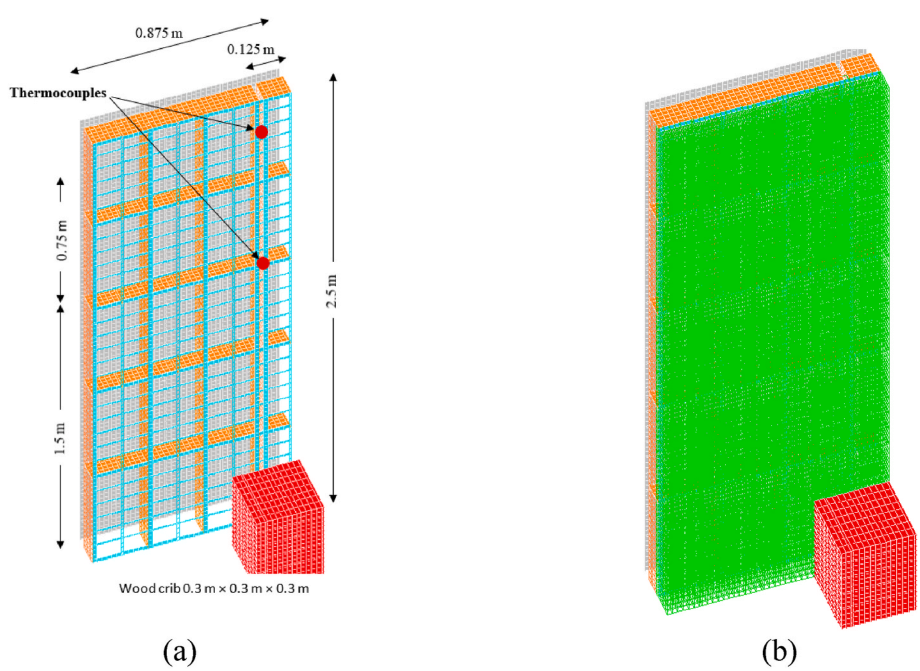

Fig. 5. Left half geometry of (a) the LW support structure and (b) the full LW system of the large-scale tests.

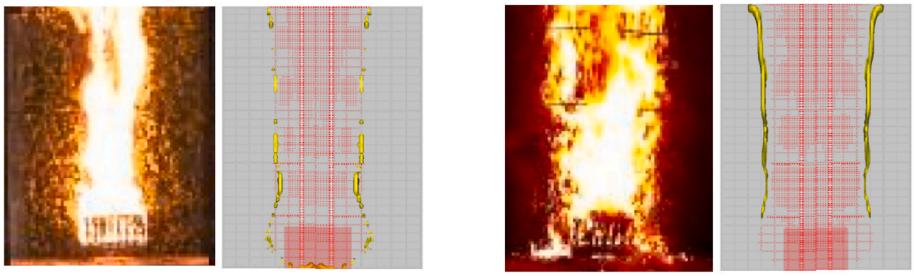

(a) (b)

Fig. 6. Observed fire plume [33] and predicted burning locations of PP (represented by red dots) and plants (represented by an iso-surface of combustion intensity of 0.36 MW/m^3 contributed by burning plants) at (a) 445 s for the wet LW test and (b) 450 s for the dry LW test. (For interpretation of the references to colour in this figure legend, the reader is referred to the Web version of this article.)

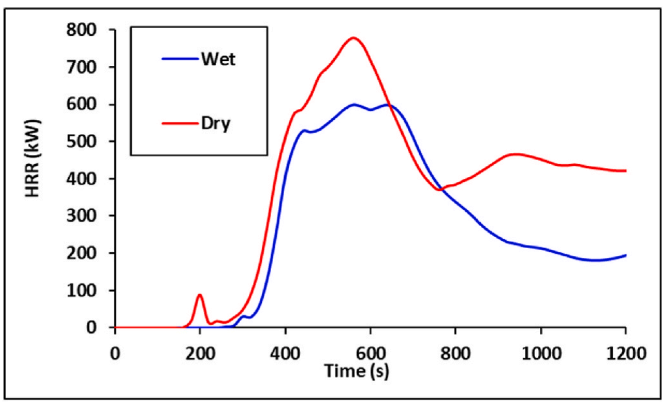

Fig. 7. The predicted HRRs from the simulation of the large-scale LW fires.

replaced.

5.1. *The fire test*

To assess the fire performance of a polymeric LW structure system, the FPA conducted a BS 8414 test in a facility that is in accordance with the 2020 BS8414 protocol [4]. As seen in Fig. 9(a), the walls of the test facility are 9.7 m high. The LW modules were only installed on the main wall and extended to a height of 5.14 m from the top of the fire chamber, which is just 0.14 m above the location of the level 2 thermocouples. The LW structure consisted of 10 module columns. There were 14 modules within each of the two columns either side of the fire chamber and 10 modules in the other columns. The modules were made of PP with the same dimensions as described in Section 3. A 0.068 m diameter PVC pipe is installed between the first and second right module columns. A PVC gutter was installed just above the top of the fire chamber with a clearance of 0.05 m from the front of the LW modules. A stack of 10 0.025-m-diameter PVC irrigation pipes was installed at the edge of the left module column. The irrigation pipes were not charged with water. A waterproof membrane was installed on the solid wall. The temperatures at level 1 and level 2 were recorded in the fire test. The temperature just before the start of ignition was 15 ^{O}C.

5.2. *Simulation setup*

The computational domain of the BS 8414 test is shown in Fig. 9(b). The CFD setup of the FPA LW BS8414 test is similar to that in the SBI fire simulation described in Section 3 and the large-scale fire in Section 4 but without the plants and growing medium. The HRR for PP is the same as that used in the previous simulations. The PVC HRR is simply approximated as 100 kW/m^2 referring to the work by Hischler M. [30]. The HRR for membrane is from the work by Blomqvist et al. [31]. Using a fine mesh at the LW structure and a relative coarse mesh at remote locations, a computational mesh consisting of 1,075,536 (660 × 168 × 97) cells is used in the simulations. The wood crib fire in this test develops faster than that observed in the DCLG cladding fires [10]. The same peak HRR of 2.5 MW as used by Wang et al. [10], is used to characterise the wood crib fire, but with a more rapid development time, i.e. 340 s to reach the peak HRR is used. Compared with the fine mesh for the previous SBI and the large simulation cases (with meshes varying from 0.01 m to 0.03 m), the mesh for the LW in the BS 8414 scenario varies between 0.017 m and 0.05 m with 0.05 m in the vertical direction. The use of a relative coarse mesh for the BS 8414 simulation is justified due to the involvement of a large fire source. Furthermore, the use of these mesh densities has been validated previously in simulations of seven cladding fires [10]. The general properties of PP, PVC and the membrane material are provided in Table 2.

5.3. *Simulation results*

Fig. 10 compares the measured and predicted external temperatures. It is important to note that the start time (i.e., zero time) in Fig. 10 for the BS 8414 test and corresponding simulation is not the time when the wood crib is ignited. It is given by a time t_s, when the temperature

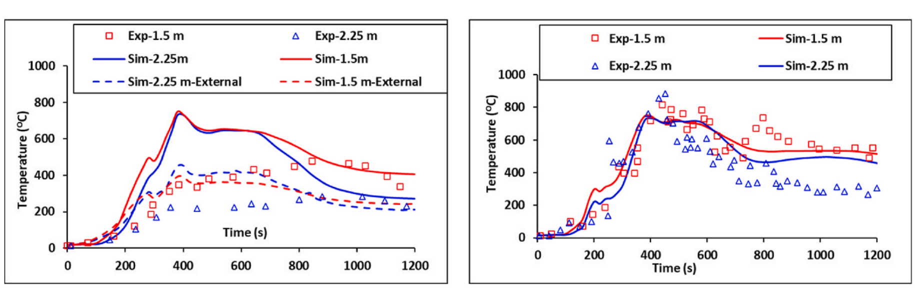

(a) (b)

Fig. 8. Predicted and measured temperatures for the large-scale tests with (a) wet and (b) dry plants.

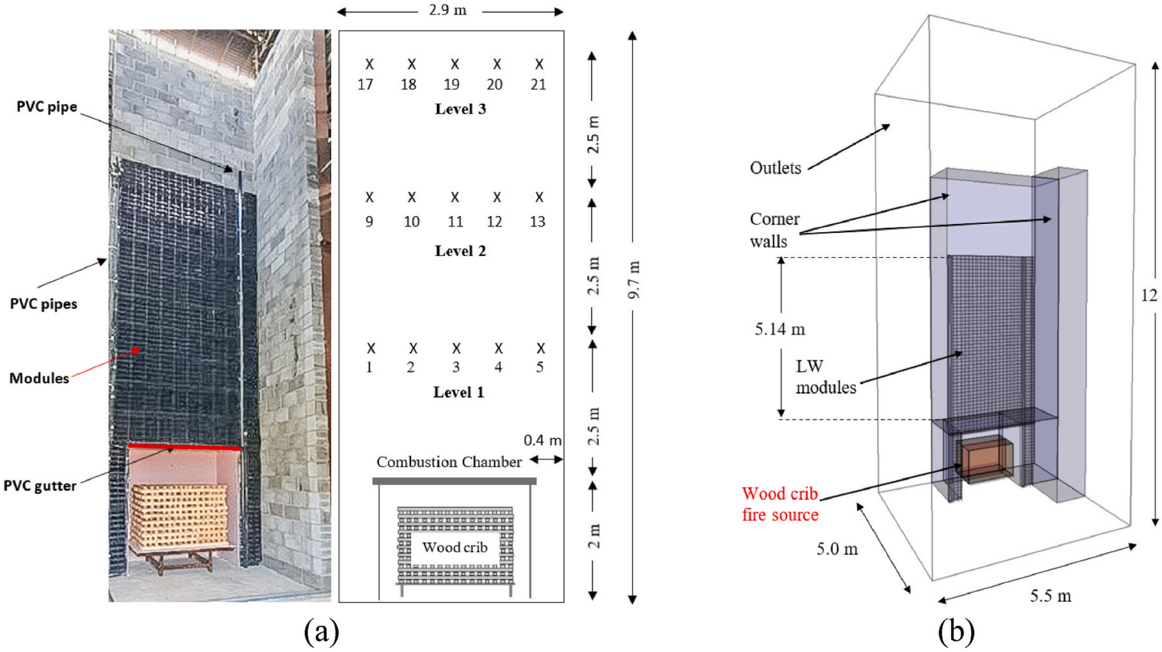

Fig. 9. BS 8414 test of LW structure (a) experimental setup and configuration of the main wall instrumentation [6] and (b) the CFD computational domain.

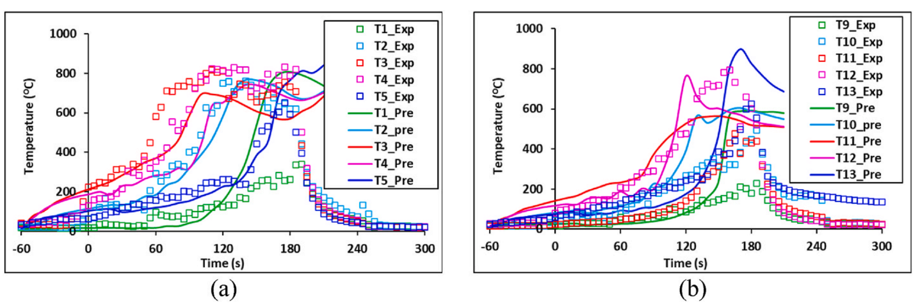

Fig. 10. Predicted and measured temperatures at (a) level 1 and (b) level 2 thermocouples.

recorded by any external thermocouple at Level 1 equals or exceeds a 200 ^{O}C temperature rise above the start time temperature and remains above this value for at least 30 s (see Fig. 10(a)). As seen in Fig. 10(a), the predicted temperatures at each thermocouple at level 1 follow the measured trends reasonably well, except at thermocouple T1. At thermocouple T1, the predicted temperature is much higher than the measured data when the fire was extinguished at 180 s. The over prediction of the temperature at thermocouple T1 is due to the early ignition of the LW modules at the left side of the fire chamber (see Fig. 11 (c)). The predicted temperatures at level 2 are also comparable with the measured data except at thermocouple T1. The rise of the temperature among the five level 2 thermocouples exceeds 600 ^{O}C at 130 s, which means that the LW structure fails the test referring to the pass/fail criteria documented in BR 135 [35]. The predicted time to fail

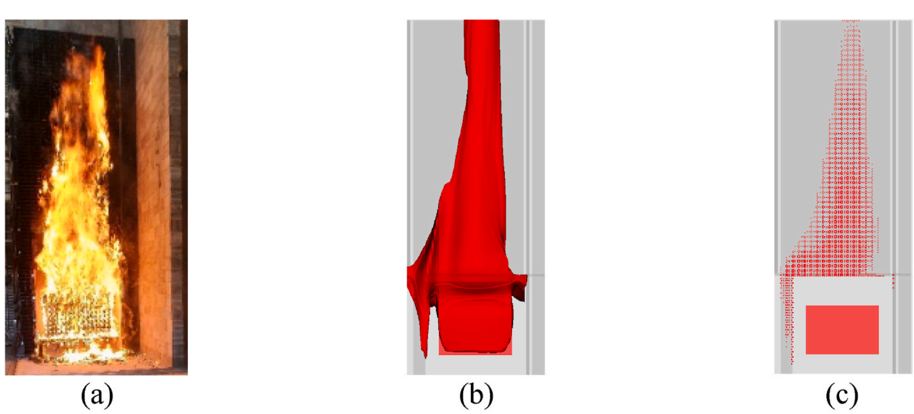

Fig. 11. (a) observed [6] and (b) predicted fire plume and (c) predicted burning locations of the LW structure at 120 s, i.e. approximately 1 min before the fire was extinguished.

is 10 s sooner at approximately 120 s. Fig. 11 visually compares the observed fire plume and predicted flame and burning locations at 120 s, approximately 1 min before the fire was extinguished.

6. Discussion

6.1. Comparison of the fire risk associated with a LW and ACM cladding with PE core

In this section, a hypothetical BS 8414 scenario is simulated using a LW structural configuration based on the FPA test [6] but with wet plants and growing medium included as in the experiments by Bielawskiet al. [20]. The fire risk posed by the hypothetical LW system is then assessed by comparing its performance with that of the BS 8414 performance of a cladding system consisting of ACM with PE core and PIR insulation. In the simulation of the LW structure BS 8414 test in Section 5 (i.e., without plants or growing medium), the predicted time to fail for the structure is 120 s. When wet plants and growing medium are included, the LW system is predicted to fail at approximately 225 s due to the external temperature at level 2 (see Fig. 12), 105 s later than the same structure without plants or growing medium. In Fig. 12, the first peak temperature of 527 ^{O}C at 115 s is the result of the plants burning around the level 2 thermocouple location. As the simulated temperature is output every 10 s, it is possible that the temperature may temporarily exceed 600 ^{O}C at around 115 s due to the burning plants. However, this elevated temperature would be sustained for just a few s while the localised plants are burning and would not constitute a failure according to the criteria in BR 135 [35] (which requires a temperature rise in excess of 600 ^{O}C for at least 30 s).

Fig. 13 depicts the predicted HRRs from BS 8414 simulations of the LW with and without plants and growing medium from the current study and an ACM cladding system (with PE core and PIR insulation) derived from simulations by Dréan V. et al. [36] and Wang et al. [10]. The start time (i.e., zero time) in Fig. 13 is not the time when the wood crib is ignited. It is given by a time t_s, when the simulated temperature at any external thermocouple at Level 1 equals or exceeds a 200 ^{O}C temperature rise above the start time temperature and remains above this value for at least 30 s. From the gradients of the HRR curves, it is clearly seen that the hypothetical LW system used in this study (with plants and growth medium) has a fast fire development similar to that for the ACM cladding with PE core simulated by Dréan et al. [36] and Wang et al. [10]. The predicted HRR for the LW system at the failure time (i.e., 225 s) is 1.24 MW. In comparison, the predicted HRR for the cladding system at its failure time (i.e., 360 s) is 1.32 MW in the simulation by Wang et al. [10]. It is approximately 1.18 MW in the simulation by Dréan et al. [36]. Thus, at their respective predicted failure times, both the LW system and the ACM cladding with PE core and PIR insulation are predicted to generate similar HRRs. Furthermore, based on modelling results, the LW system is predicted to fail some 120 s sooner than the ACM cladding system with PE core and PIR insulation i.e., 225 s compared to 360 s. Thus, overall, the fire risk posed by the hypothetical LW system is at least as high as that for an ACM cladding system with PE core and PIR insulation.

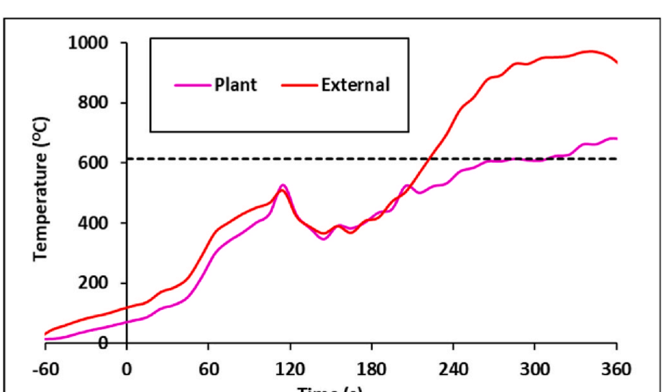

Fig. 12. Predicted maximum level 2 temperature at locations within the plant region and at external locations 0.05 m from the front face of the plants.

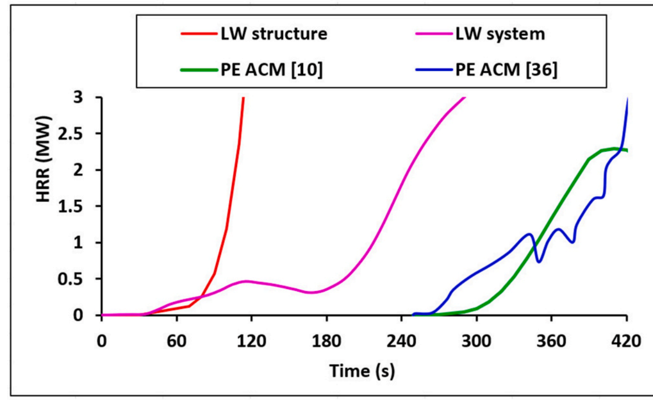

Fig. 13. Predicted HRR_S in simulations of BS 8414 test involving LW structure, LW system, and ACM cladding with PE core and PIR insulation.

6.2. Limitations

The dripping and physical failing and falling of debris are not currently considered within the model. The melting and dripping of PP and the falling of debris were observed in the FPA BS 8414 LW structure fire test, in which plants or growing medium are excluded [6]. For the fire tests involving the entire LW system [20], the involvement of plants resulted in the falling of pots and pieces of substrate. These fire behaviors are complex and beyond the capabilities of the current modelling approaches.

The simple treatment of the combustion of the complex soil and its moisture content in this study might limit the model prediction precision. As seen in Fig. 4(a), the model fails to reproduce the second peak HRR in the SBI test for the wet LW. However, a secondary peak HRR is observed in the simulation of the dry large LW fire but not the wet case (Fig. 7).

The BS 8414 simulation of the LW system utilises a wood crib burning rate derived from the FPA LW structure fire test (see Section 5.2) and as a result, the predicted time to fail is limited by the imposed wood crib burning rate. It is noted that the wood crib burning rate imposed in the FPA LW structure fire simulations is different (i.e., burns faster) to that derived for the BS 8414 DCLG fire tests [10].

The pyrolysis approach to the solid LW structure in this study uses a prescribed burning rate, which is derived from cone calorimeter tests. 50 kW/m^2 is a typical heat flux used in fire analysis at a solid fuel surface as suggested in reports by NIST [37] and SP [38]. Also, the burning behaviour of 30 tested materials in the ISO9705 tests are well correlated to cone calorimeter test data with external heat flux of 50 kW/m^2 [39]. Therefore, HRRs used in our simulations are those from cone calorimeter tests at an irradiance level of 50 kW/m^2. While this pyrolysis approach has been widely used in fire spread simulations especially for large-scale cases, in which fine meshes are impractical due to high computational cost [10,36,40,41], the adopted approach does not adapt to varying local fire conditions. Recently, Floyd and Hodges [42] proposed a pyrolysis method that utilises cone calorimeter data from multiple heat flux exposures for the calculation of burning rate, which potentially adapt the varying local fire conditions. The HRRs of PP used in the simulations are derived from cone calorimeter tests, in which the PP samples are directly exposed to the heating cone. The use of the HRR of PP from calorimeter test would be impacted by the type of growing medium filled in the modules. The model will benefit from cone calorimeter experimental data involving the burning of plastic modules filled with growing medium.

Furthermore, as discussed in Section 3.3, a 50% increase in the surface ignition temperature delays the fire spread and reduces the peak HRR by 33%. This implies that the model's flame spread results hinge on both the ignition criteria and the varying local conditions of the solid surface such as the received heat flux.

7. Conclusions

In the aftermath of the Grenfell Tower fire tragedy, there has been renewed interest in assessing the fire performance of high-rise building cladding systems including LWs. This study has presented a unique CFD fire model capable of simulating complete LW system fires by integrating a cladding fire model and a shrub-fuel-bed model using the SMARTFIRE simulation software. The shrub-fuel-bed model treats the plants and growing medium as groups of solid particles, which are characterised by a set of physical properties including density, ratio of surface area to volume and moisture content etc.

The LW fire model has been validated using data from one SBI test, two large-scale fire tests with wet and dry plants and one BS 8414 test involving only the LW structure (without plants or growth medium). The model has been shown to be able to reasonably predict the burning rate of a LW system. While the HRR from the burning of plants are sensitive to its moisture content, the surface area volume ratio and the mass, the impact on the overall peak HRR of the entire LW system is minor. The model has captured the different fire developments of the large-scale test between wet and dry LWs and produced comparable temperatures with the measured data. The model has also reproduced comparable temperatures at individual thermocouple locations in a LW structure BS 8414 test. The observed time to fail of the LW structure of 130 s is under predicted by 10 s.

A significant finding from this study is that the fire risk associated with the hypothetical LW system explored in this study (i.e., constructed of PP with wet plants and growth medium) is at least as high as that for an ACM cladding system with PE core and PIR insulation. Furthermore, the presence of wet plants and growth medium can significantly delay the time to failure of a LW system, increasing the failure time from 120 s for the LW structure without plants and growing media to 225 s for the LW system, an increase of 87%. In addition, the predicted peak HRR for the LW system with dry plants was 11% higher than that for the LW system with wet plants. It is thus recommended that fire testing of a LW system should be representative of the minimum acceptable condition of the installed system (plants and growing medium, including moisture levels), rather than the optimal condition.

Another important finding resulting from the simulations is that the HRR from the burning of the investigated LW system is mainly due to the burning of the plastic structure, not the plants and the growing medium. In the simulation of the SBI test, the predicted peak HRR from the burning of the plants is 12.9 kW, which is just 5.3% of the peak HRR of 214.4 kW for the whole LW system. This suggests that the fire risk associated with LW systems can be significantly reduced through the use of materials of limited combustibility in the construction of the LW structure. However, while not contributing significantly to the overall HRR of the LW fire, plants within the LW may be able to propagate fire to vulnerable parts of the building façade remote from the point of fire origin.

Dripping fuel losses that contribute to the flame sheet, whilst dropping, are beyond the capabilities of the current modelling approaches. The model will benefit from experiments involving the burning of the plastic modules filled with dry growing medium. Furthermore, the impact of irrigation on the LW fire development will be explored in future research.

Finally, if the BS 8414 test protocol is to be used for LW systems (i.e., including plants and growing media) it is recommended that three sets of level 2 thermocouples are included, those within the cavity, an additional set within the centre of the plant region (midway between the outer surface of the support module and the outer surface of the foliage), and the external set, 0.05 m clear of the foliage.

CRediT authorship contribution statement

Fuchen Jia: Writing – review & editing, Software, Methodology, Investigation, Formal analysis. **Zhaozhi Wang:** Writing – review & editing, Writing – original draft, Visualization, Methodology, Investigation, Formal analysis, Data curation. **Edwin R. Galea:** Writing – review & editing, Resources, Project administration, Methodology, Investigation, Funding acquisition, Formal analysis, Conceptualization. **John Ewer:** Writing – review & editing, Software, Investigation, Formal analysis.

Declaration of competing interest

The authors declare that they have no known competing financial interests or personal relationships that could have appeared to influence the work reported in this paper.

Acknowledgements

This research was supported and part funded by the University of Greenwich Innovation fund 2023 (1-R1110-321D-P13436). The authors gratefully acknowledge Wojciech Węgrzynski from Instytut Techniki Budowlanej for discussing and sharing information concerning the SBI and large-scale LW tests presented in this paper, and the Fire Protection Association (FPA) and AXA Insurance for providing the BS 8414 test data for a LW structure.

References

[1] G. Grant, D. Gedge, Living Roofs and walls from policy to practice, 10 years of urban greening, in: London and Beyond, Published by the European Federation of Green Roof and Green Wall Associations (EFB) and Livingroofs.Org on Behalf of the, Greater London Authority, 2019. https://livingroofs.org/wp-content/uploads/2019/04/LONDON-LIVING-ROOFS-WALLS-REPORT-2019.pdf. (Accessed 15 August 2022).
[2] B. Kotzen, E.R. Galea, S. Mosco, Z. Wang, J. Ewer, F. Jia, Fire safety risks of external living walls and implications for regulatory guidance in England, Fire Saf. J. 139 (2023), https://doi.org/10.1016/j.firesaf.2023.103816.
[3] BS EN 13823:2020 Test for a Single Burning Item, Reaction to Fire Tests for Building Products — Building Products Excluding Floorings Exposed to the Thermal Attack by a Single Burning Item, British Standards Institution, 2020.
[4] British Standards Institute, BS 8414-1:2020, Fire Performance or External Cladding Systems - Part 1: Test Method for Non-loadbearing External Cladding Systems Fixed To, and Supported By, a Masonry Substrate, British Standards Institute, London, 2020.
[5] Approved Document B: Fire safety- Volume 2, Buildings Other than Dwelling, 2020, p. 204. London ISBN 978 1 914124 03 7.
[6] T. Morris, Green Wall Large Scale Substructure Testing, Test Report Reference Number 103483, Fire Protection Association, 2023.
[7] K. Dahanayake, Y. Yang, Y. Wan, S. Han, C.L. Ckow, Study on the fire growth in underground green corridors, Build. Simulat. 13 (2020) 627–635, https://doi.org/10.1007/s12273-019-0595-4.
[8] T. Karunaratne, C. Chow, Fire spread along vertical greenery systems from window ejected flame: a study based on a fire dynamic simulator model, J. Build. Eng. 62 (2022), https://doi.org/10.1016/j.jobe.2022.105359.
[9] T. Karunaratne, S. Han, D. Lau, C.L. Chow, Experimental and numerical investigation of fire hazard of vertical greenery systems, J. Build. Eng. 95 (2024), https://doi.org/10.1016/j.jobe.2024.110004.
[10] Z. Wang, F. Jia, E.R. Galea, J. Ewer, CFD simulation of the BS 8414 test for cladding applications, Fire Saf. J. 153 (2025), https://doi.org/10.1016/j.firesaf.2025.104366.
[11] J. Ewer, F. Jia, A. Grandison, E.R. Galea, M.K. Patel, SMARTFIRE V4.4 User Guide and Technical Manual, FSEG, University of Greenwich, UK, 2017.
[12] F. Jia, M.K. Patel, E.R. Galea, A. Grandison, J. Ewer, CFD fire simulation of the swissair flight 111 In-flight fire – part II: fire spread within the simulated area, The Aeronautical Journal of the Royal Aeronautical Society 11 (2006) 303–331, https://doi.org/10.1017/S0001924000013178.
[13] E.R. Galea, Z. Wang, A. Veeraswamy, F. Jia, P.J. Lawrence, J. Ewer, Coupled fire/evacuation analysis of station nightclub fire, in: Proc of 9th IAFSS Symp, Sep. 21-26, 2008, pp. 465–476. Karlsruhe, Germany.

[14] E.R. Galea, L. Filippidis, Z. Wang, J. Ewer, Fire and evacuation analysis in BWB aircraft configurations: computer simulations and large-scale evacuation experiment, Aeronaut. J. 114 (2010) 271–277, https://doi.org/10.1017/S0001924000003717.

[15] E.R. Galea, Z. Wang, F. Jia, P.J. Lawrence, J. Ewer, Fire safety assessment of Open Wide Gangway underground trains in tunnels using coupled fire and evacuation simulation, Fire Mater. 41 (2016) 716–737, https://doi.org/10.1002/fam.2413.

[16] Z. Wang, F. Jia, E.R. Galea, J.H. Choi, A forensic analysis of a fatal fire in an indoor shooting range using coupled fire and evacuation modelling tools, Fire Saf. J. 91 (2017) 892–900, https://doi.org/10.1016/j.firesaf.2017.03.029.

[17] E.R. Galea, Z. Wang, F. Jia, Numerical investigation of the fatal 1985 Manchester Airport B737 fire, Aeronaut. J. 121 (2017) 287–319, https://doi.org/10.1017/aer.2016.122.

[18] B.F. Magnussen, B.H. Hjertager, On mathematical modelling of turbulent combustion with special embassies on soot formation and combustion, in: 16th Symp. (Int.) on Combustion, the Combustion Institute, 1977.

[19] Z. Wang, F. Jia, E.R. Galea, J. Ewer, Computational fluid dynamics simulation of a post-crash aircraft fire test, J. Aircraft 50 (2013), https://doi.org/10.2514/1.C031845.

[20] J. Bielawski, B. Papis, G. Krajewski, W. Wegrzynski, An exploratory investigation into moisture content and wind impact on the fire behaviour of modular living walls, Fire Saf. J. 142 (2024), https://doi.org/10.1016/j.firesaf.2023.104024.

[21] D. Morvan, J. Dupuy, Modeling of fire spread through a forest fuel bed using a multiphase formulation, Combust. Flame 127 (2001) 1981–1994, https://doi.org/10.1016/S0010-2180(01)00302-9.

[22] D. Morvan, J. Dupuy, Modeling the propagation of a wildfire through a Mediterranean shrub using a multiphase formulation, Combust. Flame 138 (2004), https://doi.org/10.1016/j.combustflame.2004.05.001.

[23] M. Newcomer, Study on the Burning Behaviour of Green Walls with Reduced Moisture Content, Master thesis, University of Edinburgh, 2022.

[24] W.J. Parker, Prediction of the heat release rate of douglas fir, International Association for Fire Safety Science (1989) 337–346.

[25] R. Susott, Characterization of the thermal properties of forest fuels by combustible gas analysis, For. Sci. 2 (1982) 404–420.

[26] L. Shi, M. Chew, Fire behaviors of polymers under autoignition conditions in a cone calorimeter, Fire Saf. J. 61 (2013), https://doi.org/10.1016/j.firesaf.2013.09.021.

[27] Babrauskas V., Ignition Handbook, Table 16, 2003, Fire Science, WA 98027, USA.

[28] Rengel B., Dréan V., Guillaume E., A preliminary numerical assessment of the interaction between ESFR sprinklers and smoke control systems in high-rack warehouses, Proceedings of Interflam 2025, Volume 1, 16th International Fire Science & Engineering Conference, 30th June – 2nd July 2025, Royal Holloway University of London, UK.

[29] G. Chai, G. Zhu, J. Zhou, Y. Gao, Y. Zhou, Y. Wang, Experimental study on burn through properties of PVC membrane room under fire, Case Stud. Therm. Eng. 26 (2021), https://doi.org/10.1016/j.csite.2021.101212.

[30] M. Hischler, Heat release from plastic materials, in: V. Babrauskas, S. Grayson (Eds.), Heat Release in Fires, Champan & Hall, 1996.

[31] P. Blomqvist, M. Hjohlman, Fire tests with textile membranes on the market - results and method development of cone calorimeter and SBI test methods, SP Report 23 (2010). ISBN 978-91-86319-61-8, ISSN 0284-5172SP, Technical Research institute of Sweden.

[32] N. Cheney, J. Gould, W. Catchpole, The influence of fuel, weather and fire shape variables on fire spread in grasslands, Int. J. Wildland Fire 3 (1993) 1993, https://doi.org/10.1071/WF9930031.

[33] J. Bielawski, B. Papis, G. Krajewski, W. Wegrzynski, Supplementary data to paper: an exploratory investigation into moisture content and wind impact on the fire behaviour of modular living walls, Fire Saf. J. 142 (2024), https://doi.org/10.1016/j.firesaf.2023.104024.

[34] J. Bielawski, Experimental investigation of moisture content influence on the fire behavior of modular living walls, in: SFPE 23 European Conference & Expo on Fire Safety Engineering, 29-30 March, 2023. Berlin, Germany.

[35] S. Colwell, T. Baker, Fire Performance of External Thermal Insulation for Walls of Multistorey Buildings, IHS BRE Press, UK, 2013, 3rd version, Watford.

[36] V. Dréan, B. Girardin, E. Guillaume, T. Fateh, Numerical simulation of the fire behaviour of facade equipped with aluminium composite material-based claddings-model validation at large scale, Fire Mater. 43 (2019) 981–1002, https://doi.org/10.1002/fam.2759.

[37] W. Grosshandler, N. Bryner, D. Madrzykowski, K. Kuntz, Report of the Technical Investigation of the Station Nightclub Fire, vols. I-II, National Institute of Standard and technology, Gaitherburg, MD., USA, 2005. NIST NCSTAR 2.

[38] M. Hjohlman, M. Försth, J. Axelsson, Design Fire for a Train Compartment, SP Report 2009:08, Fire Technology, SP Technical Research Institute of Sweden, 2009.

[39] A.S. Hansen, P.J. Hovde, Prediction of time to flashover in the ISO 9705 room corner test based on cone calorimeter test results, Fire Mater. 26 (2002) 77–86, https://doi.org/10.1002/fam.788.

[40] X. Dai, A. Gamba, C. Liu, J. Anderson, M. Charlier, D. Rush, S. Welch, An engineering CFD model for fire spread on wood cribs for travelling fires, Adv. Eng. Software 173 (2022), https://doi.org/10.1016/j.advengsoft.2022.103213.

[41] L. Jiang, A. Bøe, T. Li, Numerical simulation of fire spread in a large-scale open CLT compartment, Fire Saf. J. 150 (2024), https://doi.org/10.1016/j.firesaf.2024.104289. Part B.

[42] J. Floyd, J. Hodges, An approach for flux and thickness scaling of cone calorimeter data for predicting the pyrolysis of materials, Fire Technol. 61 (2025), https://doi.org/10.1007/s10694-025-01767-1.